

A Comparison of Cathodic Protection Parameters with High-Strength Pipeline Steels in Soil Solution

Xinhua Wang^{*}, Cui Wang, Xinghua Tang, Zhenzhen Guo

College of Mechanical Engineering and Applied Electronics Technology, Beijing University of Technology, Beijing, 100124, China

*E-mail: wangxh103@163.com

Received: 22 September 2014 / Accepted: 17 October 2014 / Published: 28 October 2014

Cathodic protection is usually used to control the corrosion in service pipeline. The optimum cathodic protection potential (OCP) becomes a vital part in order to get the best protective effect in the whole research of cathodic protection. Up to now, the OCP is often defined between 200mV to 300mV more electronegative than the free corrosion potential under usual circumstance (neutral aqueous solution or soil). However, the phenomena of over-protection and under-protection usually occur in service pipeline. The cathodic protection parameters of pipeline steel X65, X80 and X100 pipeline steel in Dagang simulated soil solution have been investigated by using the polarization test and AC electrochemical impedance spectroscopy (EIS) measurements. The values of charge transfer resistance (R_t) by analyzing the EIS curves at various cathodic protection potentials show that the polarization resistance of the specimen has a maximum value with negative shift of the polarization potential. The value is negative to $1000 \Omega \cdot \text{cm}^2$, hydrogen evolution reaction will occur. The potentials of hydrogen evolution of X65, X80 and X100 in Dagang simulated soil solutions increase orderly. The study on cathodic protection parameters of X65, X80 and X100 pipeline steels in simulated soil solution have greatly useful value and practical significance on the research about the application of transportation pipeline.

Keywords: pipeline steel; polarization curve; EIS; cathodic protection parameter

1. INTRODUCTION

Transportation pipelines are the vital industrial facilities, which can be used to satisfy the continuously raising demand for the long distance oil and gas transmission. The pipelines are manufactured in variant diameters or wall thicknesses, and they also be used to transport liquid fuels at high flow rates or high operation pressures. Transportation pipelines introduce an important economic

feasibility for oil and gas transportations, which limit the dependence on other costly approaches, such as land or sea tankers.

The researches on pipeline steel for high-pressure, large-diameter or high-grade will become a hotspot inevitable with the rapid development of oil and gas pipeline construction. What is more, new generation pipeline steels (X100/X120) attract the focuses of many researches and production institutions now [1-3]. In order to prevent corrosion and prolong the pipeline life span of in-service high-strength steel pipeline, the cathodic protections are usually applied [4-5]. However, “over protection” or “under protection” may appear easily. “Over Protection” can result in excessive cathodic hydrogen evolution and improve the susceptibility of hydrogen induced cracking significantly [6-7], while, “under protection” could not play sufficient role on the preventing of corrosion. In order to solve the two conditions above, researchers use the OCPP to take the place of the protection potential [8-10]. The OCPP is a potential that both the degree of cathodic protection and efficiency of cathodic protection current have maximum values. Under the condition of OCPP, the degree of cathodic protection and the efficiency of cathodic protection current in the protection system will coordinate with each other in the best way, and the efficiency of whole protection system will be the highest. The OCPP is often defined as 200 mV or 300 mV [11-12] electronegative than the free corrosion potential in the field or defined as the inflection point of polarization curves in laboratory tests. And both the results of the two methods are ambiguous. Tooru, [13-14] a Japanese researcher, has used EIS to determine the OCPP to prove the relationship between the OCPP and the extremum of Faraday impedance.

Many experimental works refer to X80 or some lower strength level of pipeline steel, for example, the cathodic protection parameters of X80 pipeline steel have been studied by Zhang Guohu using electrochemical technology [15]. However, there are few studies focusing on the new generation pipeline steel X100 about the cathodic protection parameters in a simulated soil solution.

The present work, as one important part of our series of studies, aimed at measuring the cathodic protection parameters of X65, X80 and X100 pipeline steels in the Dagang simulated soil solution. The results of polarization curves and EIS are used to explore the cathodic polarization behaviors of X65, X80 and X100 pipeline steels, and the cathodic protection parameters in soil simulated solution are also obtained. All the results obtained above will offer some theory and technique supports for the cathodic protection system.

2. EXPERIMENTAL SECTION

The specimens used in this work were X65, X80 and X100 pipeline steels, respectively, and the chemical compositions of them were shown in Table 1. The corresponding microstructures of them were pearlite-ferrite (X65 grade), acicular ferrite (X80 grade), particle bainite-ferrite (X100 grade), respectively. As shown in Fig. 1, the specimens were mounted in epoxy resin after de-rusting and removing oxide scale and an exposed area about 100 mm² of which were polished mechanically with finer SiC papers (400, 600, 800, 1000, 1200 grit) successively. All the specimens were degreased with acetone and distilled water and placed in a dryer to reserve after drying in a cold wind.

Table 1. Chemical compositions of X65, X80 and X100 pipeline steels (wt. %)

Pipelines	C	Si	Mn	P	S	Nb	Ti	others
X65	0.08	0.28	1.60	0.010	0.002	0.042	0.016	Mo, Cu, V
X80	0.06	0.26	1.89	0.007	0.002	0.06	0.01	Mo, Ni, Cu, Cr
X100	0.06	0.26	1.90	0.008	0.001	0.07	0.01	Mo, Ni, Cu, Cr

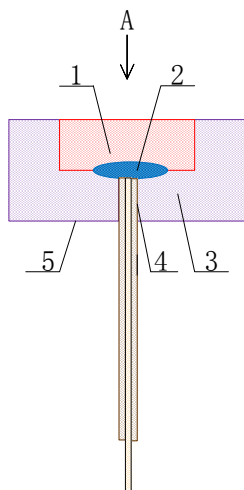


Figure 1. Schematic diagram of the electrochemical test samples: 1-specimen, 2-welding spot, 3-epoxy resin, 4-copper interconnect, 5-plastic

An alkaline soil solution has been used to simulate the soil in Dagang city, which is an important oil-producing area in China. Soil-simulating solutions were replaced the field soil to avoid uncertainty caused by impurities and other factors influence. By using analytically pure chemical reagents and deionized water for the preparation of soil solutions, according to the physicochemical properties of the soils in analysis results. Ionic concentration, chemical composition or other related parameters about Dagang soil have been listed in Table 2 or Table 3. All the experiments have been carried out at a constant temperature of 25°C.

Table 2. Ion contents in Dagang simulated soil solution (g/ L)

Ion contents	NO ³⁻	Cl ⁻	SO ₄ ²⁻	HCO ₃ ⁻	Ca ²⁺	Mg ²⁺	K ⁺	Na ⁺
Dagang	0.188	15.854	2.040	0.181	0.378	0.643	0.225	9.982

Table 3. Chemical compositions of Dagang simulated soil solution (g/ L)

compositions	CaCl ₂	NaCl	Na ₂ SO ₄	MgSO ₄ .7H ₂ O	KNO ₃	NaHCO ₃
Dagang	1.049	25.020	0.000	5.227	0.306	0.249

The electrochemical tests were carried out using the three electrode cell assembly, which was showed in Fig. 2. The specimen of X65, X80 or X100 pipeline steel, the platinum electrode and the saturated calomel electrode (SCE) were served as the working electrode (WE), the auxiliary electrode and the reference electrode (RE), respectively. The area of the auxiliary electrode was much larger than that of the working electrode, which could exert a constant potential field on the working electrode. The electrochemical cell contained about 250 mL test solution. All the potentials were reported against SCE. In order to obtain stable conditions, all experiments were set 10 minutes before starting tests.

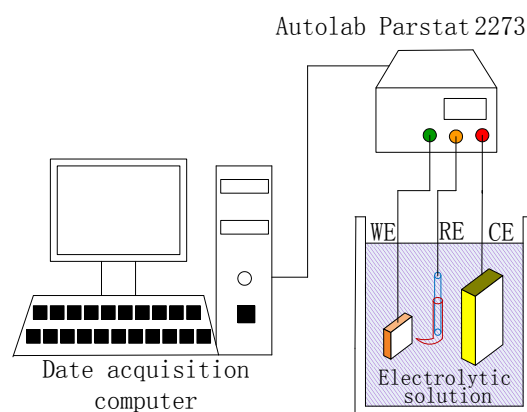


Figure 2. Electrochemical measurement device

Polarization curves and the AC impedance spectroscopy (EIS) were recorded by using a PARSTAT 2273 Integrated Test System which was controlled by one computer with a power-suit software. The cathodic polarization curves for specimens in the test solutions were recorded at a scan rate of 0.5 mV/ s. In order to find the possible range of cathodic protection potential, the potentiostatic test with a protection voltage from -1200 mV SCE to -500 mV SCE was carried out in soil-simulating condition. The testing frequency ranged from 100 KHz to 0.01 Hz, and the AC sine excitation signal was 10mV. The experimental data were evaluated and analyzed by the commercial software “Zsimpwin”.

3. RESULTS AND DISCUSSION

3.1 The polarization tests

The range of minimum and maximum protection potential can be obtained according to the polarization curves. The curves of X65, X80 and X100 steel in Dagang simulated soil solution are showed in Fig. 3 - 5, respectively.

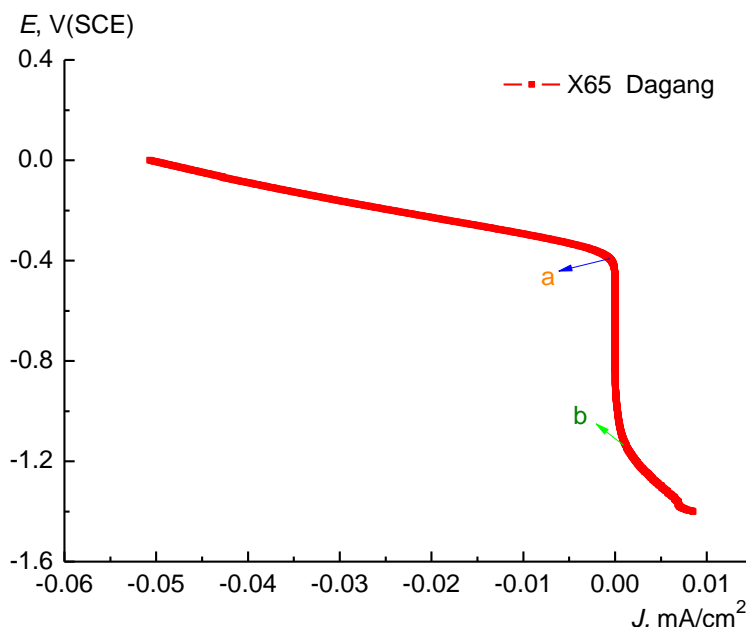


Figure 3. Polarization curve of X65 in Dagang simulated soil solution

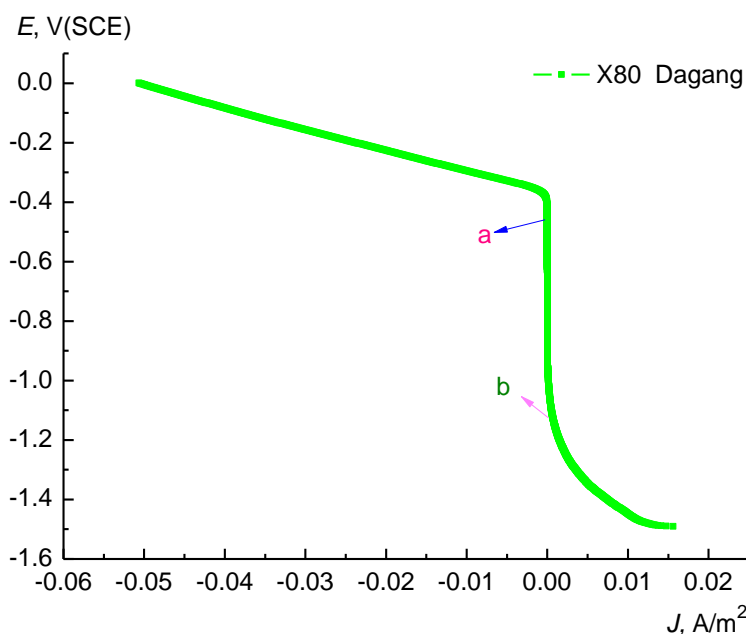
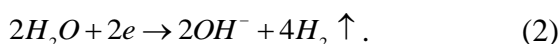


Figure 4. Polarization curve of X80 in Dagang simulated soil solution

It can be noticed that the shapes of these polarization curves are similar. Moreover, there are two obvious inflection points in all curves. A is just the point that the cathodic reaction is controlled by oxygen diffusion instead of activation. The reaction is an oxygen reduction reaction, which can be shown by equation (1), prior to point **a**. Cathodic protection can maintain the cathodic reduction of metal in a stable state by applying a current or potential, to avoid the oxidation of the surface or hydrogen corrosion. Cathodic reaction after point **b** is controlled by the hydrogen depolarization, which can be shown as equation (2)[16]:



From the three polarization curves above, it is found that the cathodic current densities tend to increase with the increase of DC electrode potential toward to the negative direction.

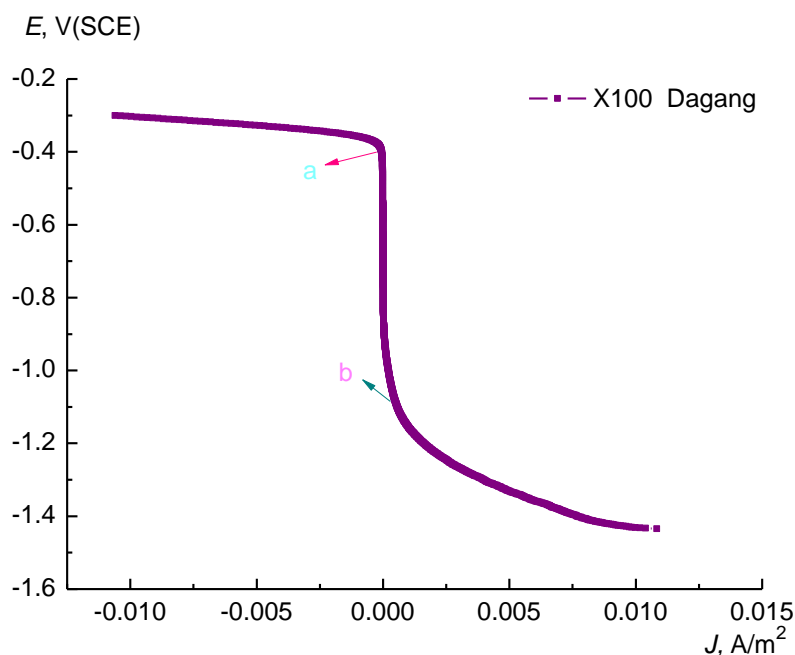


Figure 5. Polarization curve of X100 in Dagang simulated soil solution

The current density is relatively stable in the range from point a to point b. If the electrode potential is lower than the potential of point b, the cathode current will increase rapidly, and this phenomenon is attributed to that the hydrogen ion can produce during the reduction reaction and then the hydrogen ion releases from the surface of sample. Based on the results above, it can be obtained that the OCP of X65 pipeline steel in soil solution ranges from -400 mV to -1200 mV. The OCP of X80 steel specimen ranges from -400 mV to -1150 mV. Similarly, the OCP of X100 pipeline is on the scale of -380 mV to -1130 mV. Polarization tests can give the range of protection potential, which is relatively large and vague, and the accurate value of best potential needs to combine the impedance spectra of cathodic protection parameter to analysis further.

3.2 The EIS tests

In order to study the cathodic polarization behaviors of X65, X80 and X100 pipeline steel in Dagang soil solutions, EIS measurements have been performed at various cathodic polarization potentials (from -1200 mV SCE to -500 mV SCE), as shown in Fig. 6 - 8, respectively. The Nyquist plots can be divided into two parts, the high frequency parts, which reflect the information of corrosion products, are similar, while the low frequency parts are quite different. The phenomena imply that there are different electrode reactions [17]. The phenomena show that the corrosion products at the cathodic polarization potential change lightly, while the charge transfer resistance (R_t) shows a regular pattern when the cathodic polarization potential changes [18].

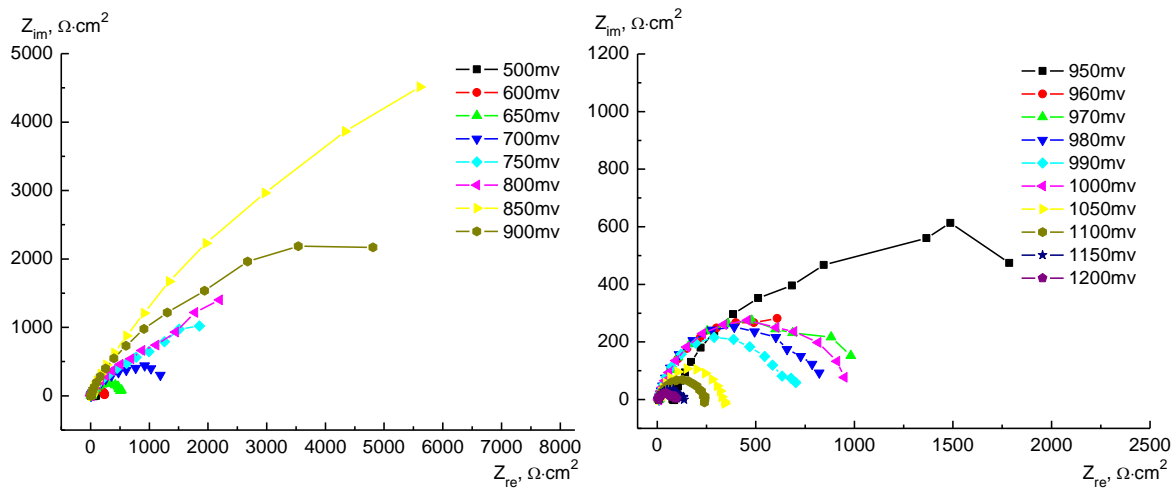


Figure 6. Effect of Nyquist plot of X65 steel at different cathodic polarization voltages

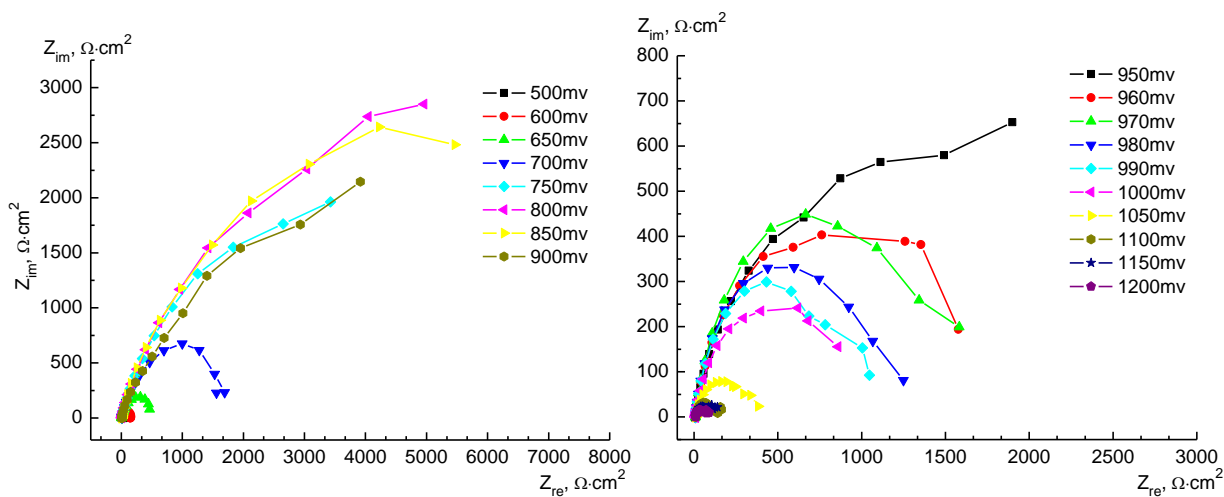


Figure 7. Effects of Nyquist plots of X80 steel at different cathodic polarization voltages

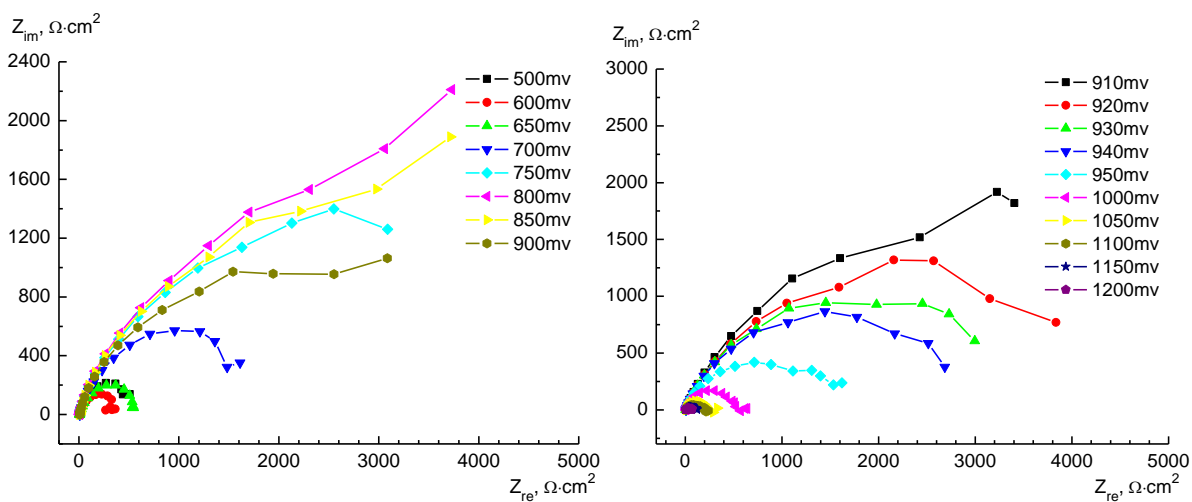


Figure 8. Effect of Nyquist plot of X100 steel at different cathodic polarization voltages

The results of EIS of X65, X80 and X100 pipeline steel at different potential in Dagang soil solution are analyzed by Zsimpwin 3.10 software, the corresponding equivalent circuits of them are proposed in Fig. 9 according to the theoretical analysis [19-20]. In Fig. 9, L means inductance and R_s means medium resistance. R_1 stands for the resistance between corrosion products and solution, while R_t is the charge transfer resistance.

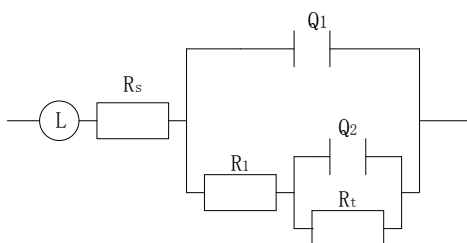


Figure 9. Equivalent circuit of the EIS

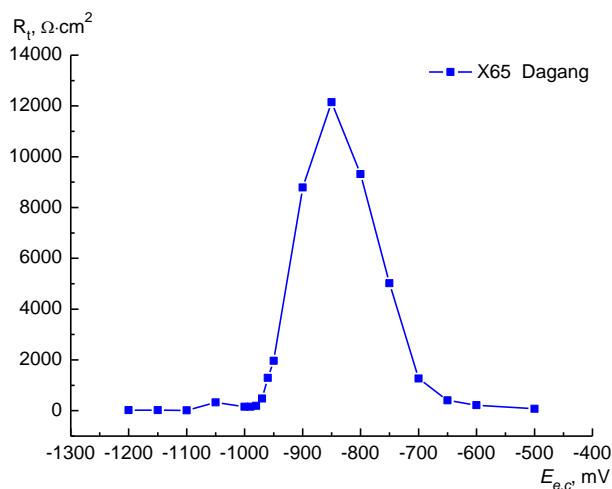


Figure 10. R_t - $E_{e,c}$ curve of X65 in Dagang simulated soil solution

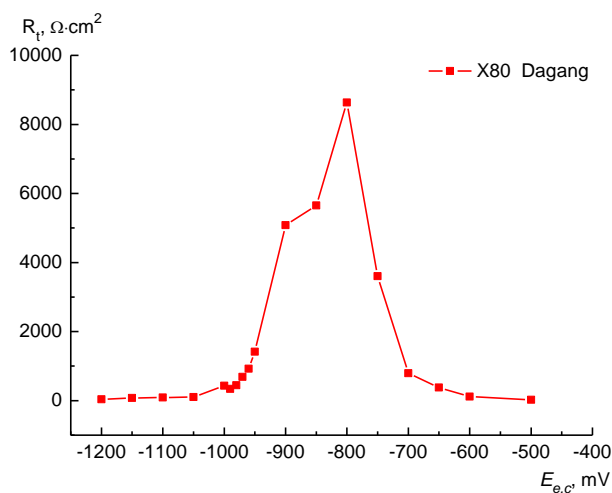


Figure 11. R_t - $E_{e,c}$ curve of X80 in Dagang simulated soil solution

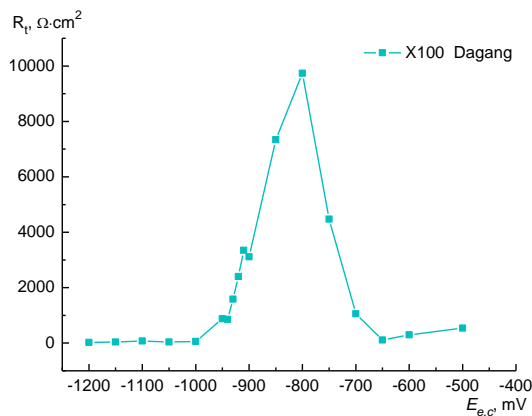


Figure 12. R_t - $E_{e,c}$ curve of X100 in Dagang simulated soil solution

Constant phase element (Q) is commonly used to replace the capacitance, because it hardly has pure capacitance in real electrochemical processes. Q_1 is the combined capacitance of product and solution, Q_2 is the double layer capacitance. The charge transfer resistance, R_t , is coincident with the Faraday impedance, R_F . The OCPP can be obtained by discussing the relationship between the Faraday impedance characteristic of the steel with impressed current cathodic protection in soil solution. The OCPP is approximate equal to the electric potential at the maximum of the Faraday impedance, R_F [21]. Based on the results of EIS, the R_t - $E_{e,c}$ curves of X65, X80, X100 in Dagang soil solution can be obtained and shown in Fig. 10 - 12, respectively.

At the open circuit potential, there are two reactions, anodic reaction and cathodic reaction. The impedance is the result of the balance between the anodic and cathodic reactions. According to the electrochemical theory [21], the analytic formula can be shown as follows:

$$1/R_t = 1/R_{t,a} + 1/R_{t,c} \tag{3}$$

Where, R_t , $R_{t,a}$ and $R_{t,c}$ stand for the charge transfer resistance of the electrode reaction, the anodic reaction, the cathodic reaction, respectively.

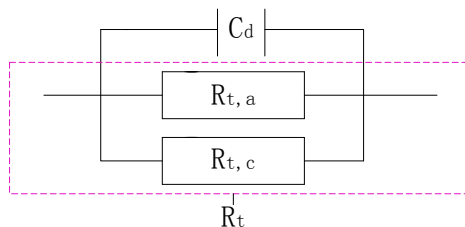


Figure 13. Equivalent circuit at OCP

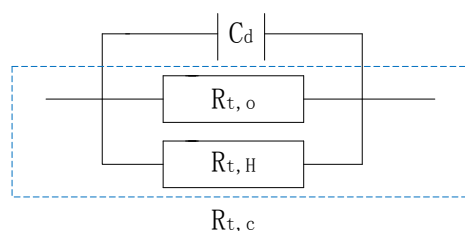


Figure 14. Equivalent circuit in polarization potential

Adding cathodic polarization to the electrodes, the value of $R_{t,a}$ will increase with the negative of potential, however, the value of $R_{t,c}$ will decline at a slow pace, which is due to the activation of oxygen electrochemical process control. The electrochemical reaction can be represented by an equivalent circuit, which is shown in Fig. 13. When the electrode potential reaches one specific point of protection potential, the reaction of hydrogen cathodic reduction will occur besides the reaction of oxygen cathodic reduction. Fig. 14 shows the equivalent circuit of the reaction in this case. Impedance spectroscopy analytical formula is listed as following:

$$1/R_{t,c} = 1/R_{t,o} + 1/R_{t,H}, \quad (4)$$

The protection degree (p) is defined by the following equation:

$$p = \frac{\text{corrosion rate at open circuit potential(OCP)} - \text{corrosion rate at CP}}{\text{corrosion rate at OCP}} \quad (5)$$

The utilization of protection current (q) is:

$$q = \frac{\text{OCP} - \text{corrosion rate at CP}}{\text{protection current}}. \quad (6)$$

Where, corrosion current stands for corrosion rate. As shown in equations (5) and (6), p increases with the negative shift, while q decreases with the negative shift. The phenomena are caused by the results that the hydrogen evolution reaction can consume cathodic protection current. The result of $p \times q$ can reflect the overall efficiency of the entire cathodic protection system, and it is defined as the actual protection efficiency by $r = p \times q$. The two parameters have opposite trends, which can lead to a maximum value of r . The potential corresponding to the maximum is OCPP. Based on literature [22], the potentials, corresponding to the maximum of r and R_t , are nearly consistent, so the OCPP is the potential that corresponding to the maximum of R_t .

The R_t - $E_{e,c}$ curve (Fig. 10) shows that R_t of X65 steel in soil solution rapidly increases and then reduces with the decreases of the cathodic polarization potential. Before reaching to the maximum point (-850 mV), the relationship between R_t and potential can be explained by equation (3), while the relationship between R_t and potential can be analyzed by equation (4) if the range is below -850 mV. When the ratio of hydrogen evolution reaction in the total cathode reaction is very small, it can be thought that $R_{t,H} \rightarrow \infty$. $R_{t,c}$ is approximately equal to the transfer resistance of cathodic oxygen reduction reaction ($R_{t,o}$). $R_{t,c}$ gradually decreases as the cathode potential negative shift. If the hydrogen evolution reaction occurs obviously in the reaction system, $R_{t,H}$ becomes smaller, and works along with $R_{t,o}$ to affect $R_{t,c}$. Due to the influence of $R_{t,H}$, $R_{t,c}$ decreases rapidly, which leads an inflection point in the R_t - $E_{e,c}$ curve. The point is the potential of hydrogen evolution corresponding to the cathodic polarization potential. Therefore, the potential of hydrogen evolution of X65 pipeline steel in soil simulated solution is -970mV and the OCPP is -850mV.

The R_t - $E_{e,c}$ curves (Fig. 11 - 12) have similar trends. R_t in soil solution rapidly increases and then reduces with the decrease of the cathodic polarization potential. The results can be obtained that the potential of hydrogen evolution and the OCPP of X80 steel are -960 mV and -800 mV, respectively. Similarly, it can be obtained that the hydrogen evolution potential and OCPP X100 pipeline steel are -940 mV and -785 mV, respectively (listed in Table 4).

Table 4. The OCPP and potential of hydrogen evolution in Dagang simulated soil solution

Pipeline steels	X65	X80	X100
OCPP	-850mV	-800mV	-785mV
Hydrogen-charged potential	-970mV	-960mV	-940mV

As shown in Table 4, the hydrogen-charged potential and OCPP of X65, X80 and X100 pipeline steel orderly increase. According to literature [23], the higher is the dislocation density of pipeline, the more prone to appear the hydrogen evolution. The corresponding microstructure is pearlite-ferrite (X65 grade), acicular ferrite (X80 grade), particle bainite-ferrite (X100 grade). Dislocation density of X100 is higher than X65 and X80, and the absolute potential of hydrogen evolution is the minimum. The results are consistent with the work.

Combining the potential of hydrogen evolution (as shown in Table 4) and the experimental phenomena, the R_t can be analyzed by calculation. It is concluded that the hydrogen evolution begins to occur (fewer bubbles precipitate) if R_t is less than $1000\Omega\cdot\text{cm}^2$, the hydrogen evolution gets to very obvious (more bubbles) if R_t is less than $600\Omega\cdot\text{cm}^2$, and the hydrogen evolution occurs violently if R_t is less than $150\Omega\cdot\text{cm}^2$. Thus, the cathode potential (R_t is less than $1000\Omega\cdot\text{cm}^2$) is the hydrogen evolution potential.

As shown in the $R_t-E_{e,c}$ curves, it can be divided into four areas, the first part is the area from the OCP to the OCPP with the largest slope, the second area is from the OCPP to the potential of hydrogen evolution with a larger slope, the third part is the origin potential of hydrogen to the potential of obvious evolution with a smaller slope, and the last one is after the obvious hydrogen reaction with a slope almost to zero.

4. CONCLUSION

The following conclusions can be made based on the results presented in this paper.

(a) The shapes of polarization curves of X65, X80 and X100 are similar with two obvious inflection points, and the potential corresponding to the second point is the potential of hydrogen evolution.

(b) The potential of hydrogen reaction and the OCPP of X65, X80 and X100 pipeline steel in soil solution increase orderly.

(c) The hydrogen evolution potential is the cathode potential (R_t is less than $1000\Omega\cdot\text{cm}^2$) according to the analysis about the potential of hydrogen evolution and the experimental phenomena.

(d) The $R_t-E_{e,c}$ curves can be divided into four areas, which are the areas from the OCP to the OCPP with the largest slope, from the OCPP to the potential of hydrogen evolution with a larger slope, from the origin potential of hydrogen to the potential of obvious evolution with a smaller slope, and after the obvious hydrogen reaction with a slope almost to zero, respectively.

ACKNOWLEDGEMENTS

This research is supported by National High Technology Research and Development Program of China (No. 2012AA040105) and National Natural Science Foundation of China (No. 51471011).

References

1. L. K. Ji, J. Z. Wu, *Oil Tubular Goods Engineering.*, 13 (2007) 48.
2. L. K. Ji, H. L. Li, Y. R. Feng, *Oil Tubular Goods Engineering.*, 13 (2007) 1.
3. X. X. Wang, *Welded Pipe and Tube.*, 35 (2012) 5.
4. A. A. Ahmed, O. H. Basim, H. A. Mohammed, *International Journal of Current Engineering and Technology.*, 3 (2013) 2016.
5. R. G. Esquivel, Q. Z. Olivares, M. J. H. Gayosso, A. G. Trejo, *Mater. Corros.*, 62 (2011) 61.
6. J. C. Barker, *Health and Safety Executive*, 1998.
7. W. L. Zhen, *Environment sensitive fracture of steel*, Beijing: Metallurgical Industry Press., 1988.
8. X. P. Guo, H. M. Zhang, Y. F. Tang, *Corrosion Science and Protection Technology*, 1 (1989) 6.
9. X. N. Xu, C. D. Zhang, *Corrosion & Protection.*, 18 (1996) 7.
10. J. X. Wu, Z. G. Fu, P. Q. Zhang, *Journal of Chinese Society of Corrosion and Protection.*, 9 (1989) 160.
11. M. Oonishi, *Boosei Kanri.*, 20 (1976) 24.
12. T. Kakehi, *Boshoku Gijutsu.*, 21 (1972) 124.
13. T. Tsuru, *Boshoku Gijutsu.*, 34 (1985) 36.
14. T. Tsuru, *Bosei Kanri.*, 30 (1986) 1.
15. G. H. Zhang, M. Gong, Q. T. Tang, X. M. Zhang, *Corrosion & Protection.*, 32 (2011) 868.
16. Q. M. Ding, Z.L. Li, H. N. Hao, *Anti-Corrosion Methods and Materials*, 6 (2013) 283.
17. M. C. Bernard, S. Joiret, A. Hugot Le Goff, *Russ. J. Electrochem.*, 40 (2004) 235.
18. M. C. Li, H. C. Lin, C. N. Cao, *Journal of Chinese Society for Corrosion and Protection.*, 20 (2000) 111.
19. Z. L. Li, Q. M. Ding, Y. F. Zhang, J. J. Li, S. L. Li, *Corrosion & Protection.*, 31 (2010) 436.
20. F. Mansfeld, *Russ. J. Electrochem.*, 36 (2000) 1205.
21. C. N. Cao, J. Q. Zhang, *An introduction to electrochemical impedance spectroscopy*, Beijing: Science Press., 2002.
22. P. R. Sere, J. D. Culcasi, C. I. Elsner, A. D. Sarli, *Surf. Coat. Technol.*, 122 (1999) 143.
23. P. Tao, C. Zhang, *Weld pipe and tube.*, 31 (2008) 19.

© 2014 The Authors. Published by ESG (www.electrochemsci.org). This article is an open access article distributed under the terms and conditions of the Creative Commons Attribution license (<http://creativecommons.org/licenses/by/4.0/>).